Catal Lett (2008) 123:269–275
DOI 10.1007/s10562-008-9418-4

Different Catalytic Reactions of *n*-Hexane and 1-Hexene on Molybdenum Based Catalysts

F. Al-Kharafi · H. Al-Kandari · A. Katrib

Received: 12 November 2007 / Accepted: 23 January 2008 / Published online: 12 February 2008

Abstract Controlled reduction by hydrogen, of the equivalent five monolayer of MoO_3 deposited on TiO_2 as a function of the reduction temperature up to 873 K, enabled us to obtain three Mo_2O_5, bifunctional (metal-acid) $MoO_2(H_x)_{ac}$ and the metallic Mo(0) phases. Characterization of these phases was made by employing surface XPS-UPS techniques in parallel with catalytic reactions. Hydroisomerization of *n*-hexane occurs on the bifunctional phase, while hydrogenation/ dehydrogenation and benzene formation were performed by the metallic Mo state.

Keywords XPS-UPS · MoO_3 · MoO_2 · TiO_2 · Al_2O_3 · Hydroisomerization of *n*-Hexane · Benzene · Toluene

1 Introduction

Identification of the active site(s), responsible for specific catalytic process(s), is a major challenge to research workers in this field. Several characterization techniques can provide general information on the bulk structure and/ or surface structure in a broad sense. However, none of these techniques can define exactly the real composition of the active chemical species present on the outermost surface layer, responsible for the catalytic activity of a given system. This is due, in part, to the fact that the catalytic activity of a given surface is obtained, in situ, under specific experimental conditions such as pressure and temperature. However, combination of XPS-UPS techniques measurements in parallel with catalytic measurements carried out at the same experimental conditions could provide valuable information concerning the electronic structure of the outermost surface layer.

Hydroisomerization of *n*-hexane to mono- and di-branched molecules is an important catalytic process in order to increase the octane number and to improve the motor engine working conditions. These catalytic processes take place in several consecutive catalytic steps, summarized in terms of a bifunctional (metal-acid) mechanism [1]. Platinum based catalysts are the most commonly used systems at the industrial and the fundamental research concerning the isomerization of light alkanes [2–4]. In these systems, the metallic function consists of finely dispersed platinum particles (few atoms), on acidic support such as chlorinated alumina. Platinum is rare and expensive. Also, there are several problems associated with the use of these catalysts such as the corrosion caused by chlorine, the poisoning of the platinum by sulfur and water, as well as the formation of toxic benzene as a by-product. As a result, possible replacement of Pt based catalysts is of great general interest. Systematic research work using different surface techniques in association with catalytic experiments enabled us to identify a new type of catalysts, having comparable performances to the best Pt catalysts [5–7]. These catalytic systems consist of molybdenum or tungsten dioxide MO_2 (M = Mo, W) species as the active species, with a bifunctional $MO_2(H_x)_{ac}$ phase as the outermost surface layer. The metallic function is attributed to the delocalized π electrons over the M–M atoms placed along the *C*-axis of the deformed rutile structure of MO_2. On the other hand, the acidic function is formed as a result of hydrogen dissociation by this metallic function followed by hydrogen atom(s) bonding to surface oxygen to produce Brönsted M–OH acidic group(s). The bifunctional

F. Al-Kharafi · H. Al-Kandari · A. Katrib (✉)
Department of Chemistry, Kuwait University, P.O. Box 5969, Safat 13060, Kuwait
e-mail: a.katrib@kuniv.edu

$MO_2(H_x)_{ac}$ phase is characterized by the Mo(3d) or W(4f) spin-orbit coupling binding energies, the oxygen 1s of the Brönsted acidic group(s), and the well-resolved π and σ bands in the UPS spectrum [8]. One important feature of this bifunctional $MoO_2(H_x)_{ac}$ phase resides in the fact that the metallic function consists of an atomic wire of the transition element M in a stable MO_2 state under experimental conditions. Consequently, different particle size(s) are not formed which might occur during the catalyst preparation and/or due to sintering problems as is the case in Pt based catalysts. In the case of molybdenum catalysts studied in this work, the stability of different Mo phases, formed at different reduction temperatures, has been tested for several days without any changes in structure and catalytic performances. Moreover, the bifunctional $MoO_2(H_x)_{ac}$ state shows considerable resistance to corrosion by sulphur and water.

2 Experimental

The equivalent of 5 monolayers of molybdenum trioxide were deposited on TiO_2 using ammonium heptamolybdate $(NH_4)_6Mo_7O_{24}.4H_2O$ (99.9%) supplied by STREM Chemicals. Titanium dioxide, TiO_2, is Degussa P-25 (25% rutile) with pore volume of 0.5 cm^3/g and BET surface area of 50 ± 5 m^2/g. Supported catalysts are prepared by impregnating the appropriate amount of molybdenum in ammonium heptamolybdate salt, following the method described by Pines et al. [9]. The prepared catalysts were calcined at 773 K for 12 h. The catalytic experiments were performed using 100 mg of the catalyst in a fixed bed quartz reactor. The catalytic experiments were conducted in a pulse mode under continuous hydrogen flow rate of 40 cm^3/min. The catalytic products were analyzed by gas chromatography using 100 m (Petrocol-DH) column and a flame ionization detector.

Characterization of the samples by XPS was conducted using VG Scientific ESCALAB-200 spectrometer. The radiation source was an Mg Kα operating at a power of 300 W (15 kV, 20 mA). UPS He(I) resonance 584 Å radiation of 21.217 eV was employed for the VB energy region measurements. Vacuum in the analysis chamber was below 7×10^{-9} mbar during all measurements. In-situ reduction was conducted in a high-pressure gas cell, housed in the preparation chamber, with hydrogen flow at 200 mL/min. Reported binding energies were based on the carbon contamination C1s at 284.8 eV within an experimental error of $\pm$ 0.1 eV.

Catalytic reactions of *n*-hexane and 1-hexene on different molybdenum surfaces will be studied as follows: Pulses of the reactant is introduced on a fresh MoO_3/TiO_2 sample as a function of reduction temperature up to 673 K. At each temperature, the sample is kept for 1 h under hydrogen. Beyond 623 K reduction temperature, the reaction temperature is maintained at 623 K. Then, the reduction time is extended to 12 h at 673 K. Consequently, catalytic reactions were studied as a function of the reaction temperature. On the basis of characterization experiments, it is expected that the sample surface is totally converted to MoO_2 with the bifunctional $MoO_2(H_x)_{ac}$ phase as the outermost surface layer. In order to verify the reproducibility of the results and the stability of the catalyst surface structure, reaction temperatures were decreased and increased up to 673 K several times. An increase in the reduction temperature beyond 673 K is expected to produce the metallic Mo(0) state on the sample surface as observed in XPS-UPS measurements. Surface structure changes as a function of the reduction temperature increase up to 873 K has been evaluated by catalytic activity tests at 623 K reaction temperature. In order to convert the upper surface monolayer(s) to the metallic Mo(0) state, the sample is kept under hydrogen flow for 24 h at 873 K. Catalytic performances of this surface have been evaluated by the injection of reactant pulses at different reaction temperatures.

2.1 Spectroscopic Characterization of the Catalysts

The XPS-UPS experiments of the MoO_3/TiO_2 before and after hydrogen reduction at different temperatures were carried out in situ in order to avoid any re-oxidation of the sample following its exposure to air. Assignment of the different molybdenum oxidation states is done based on the XPS of the Mo ($3d_{3/2,5/2}$) spin-orbit components binding energies: These values are at 235.85 and 232.65 eV for MoO_3, 234.9 and 231.7 eV for Mo_2O_5, 232.3 and 229.1 eV for MoO_2, 230.85 and 227.7 eV for Mo (0) [10]. Moreover, molybdenum dioxide is characterized by additional structure in terms of the presence of two π (0.4 eV) and σ (1.4 eV) bands in the VB energy region [8]. Additional information concerning the presence of MoO_2 phase in the upper 4–5 monolayers of the sample surface could be obtained from the UPS spectrum.

The XPS of the MoO_3/TiO_2 sample prior to any reduction treatments shows the presence of two distinct spectral lines at 235.85 and 232.65 eV, characteristics of the MoO_3 phase (Fig. 1a). There is no density of state structure (DOS) at the Fermi level (Fig. 2a). A symmetrical spectral line at 530.5 eV is attributed to the O1s of the oxide oxygen in MoO_3 and TiO_2 (Fig. 3a). The specific spectral lines of these two oxides cannot be resolved because of relatively small energy difference as compared to the X-ray line broadening. In situ sample exposure to hydrogen at temperatures up to 573 K results in the

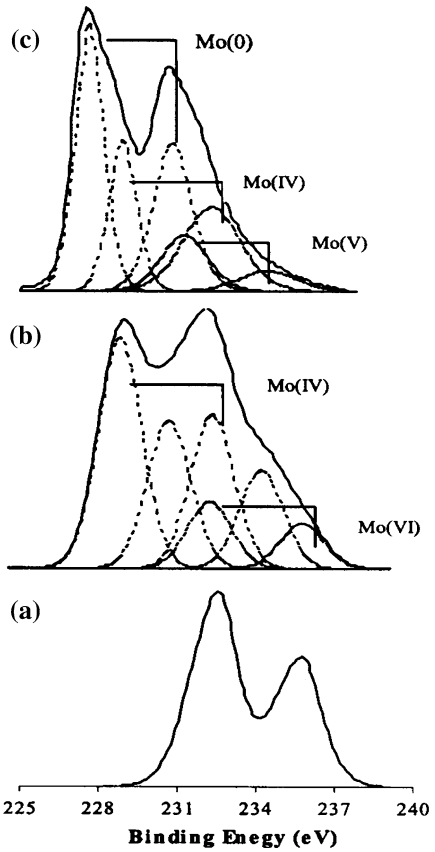

Fig. 1 The XPS of Mo (3d) in MoO_3/TiO_2, (**a**) after calcinations at 773 K, (**b**) after reduction at 673 K for 2 h, (**c**) after reduction at 873 K for 24 h

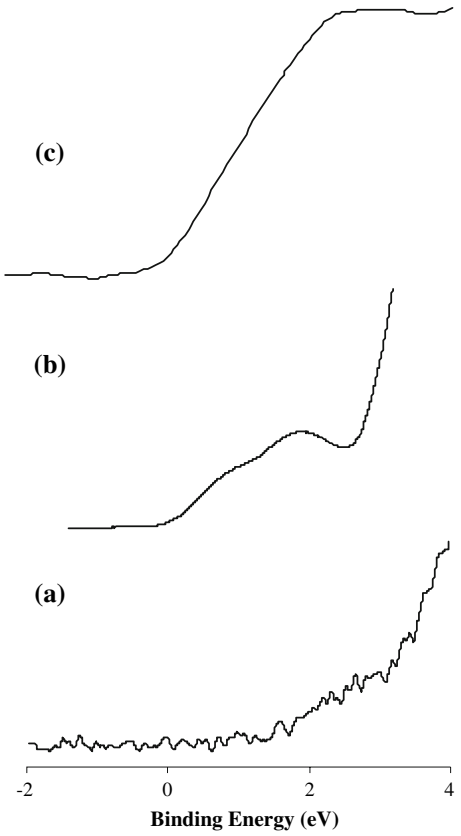

Fig. 2 The UPS of the VB in MoO_3/TiO_2, (**a**) after calcinations at 773 K, (**b**) after reduction at 673 K for 2 h, (**c**) after reduction at 873 K for 24 h

formation of Mo_2O_5 state characterized by the Mo(3d) spin-orbit components. However, an increase in the reduction temperature up to 673 K for 2 h results in the formation of MoO_2. The presence of this phase is characterized by the Mo ($3d_{3/2,5/2}$) at 232.3 and 229.1 eV (Fig. 1b) as well as the π and σ bands, measured at 0.4 and 1.4 eV (Fig. 2b). Moreover, aside from the main oxide oxygen spectral line at 530.6 eV, a shoulder at 531.6 eV (Fig. 3b) was observed. The presence of this low intensity spectral line is attributed to the presence of Brönsted Mo-OH acidic group(s) on the sample surface. The formation of these Brönsted acidic group(s) is resulted from consecutive processes in which hydrogen molecules are dissociated by the MoO_2 metallic function, followed by bonding of the produced hydrogen atom(s) to surface oxygen. The presence of both metallic and acidic functions along the Mo–Mo long chain atoms is symbolized by $MoO_2(H_x)_{ac}$ phase. Reduction to the metallic state is observed following extended exposure of the sample to hydrogen at 873 K for 24 h. The Mo(0) state is characterized by the Mo spin-orbit components at 230.85 and 227.7 eV (Fig. 1c). As could be observed from this spectrum that the reduction process at relatively high temperatures enabled to reduce part (60%) of the molybdenum oxide(s) to the metallic Mo(0) state. The presence of this metallic state on the sample surface could be confirmed from the relative increase in the DOS structure (Fig. 2c) as well as the stable metallic catalytic activity which will be discussed later. Molybdenum oxides MoO_2 and Mo_2O_5 states are still present in the sample structure, most probably located at the inter-phase between surface Mo(0) and the support. The oxygen 1s energy region in this case consists of a main spectral line at 530.5 eV and low intensity shoulder at $\sim$532.5 eV, most probably due to some adsorbed oxygen on the sample surface. Trace of oxygen impurity in the hydrogen gas employed in this reduction process could be at the origin of such adsorption. The possibility of trapped oxygen in the sample matrix following the reduction process is not excluded.

In order to get more information about the possible changes in the catalyst surface structure following its exposure to the reactant hydrocarbon/hydrogen mixture as a function of time, we have measured the XPS of $MoO_2(H_x)_{ac}$ and Mo(0) samples following its use in the catalytic experiments for several days. Observed

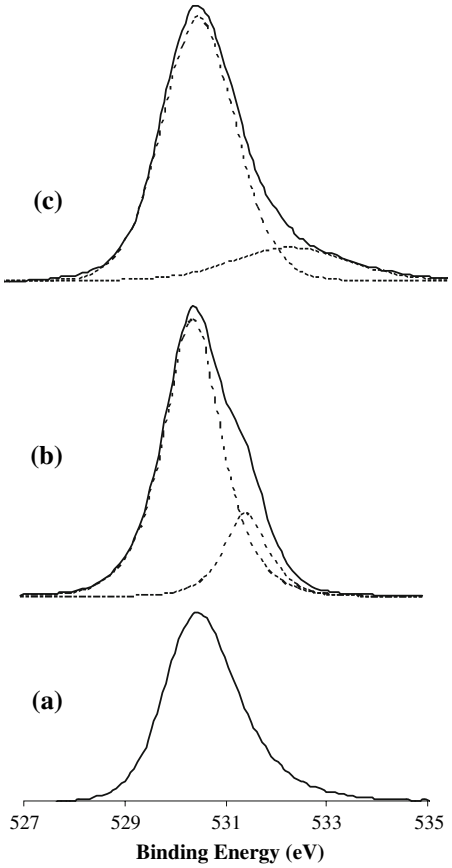

Fig. 3 The XPS of the O1s in MoO_3/TiO_2, (**a**) after calcinations at 773 K, (**b**) after reduction at 673 K for 2 h, (**c**) after reduction at 873 K for 24 h

molybdenum dioxide (Fig. 4a) is still present in the bifunctional $MoO_2(H_x)_{ac}$ state. The decrease in its relative intensity as compared to the freshly reduced, in situ, sample (Fig. 1b) is most probably due to the re-oxidation of part of the sample surface to MoO_3 following its exposure to air. On the other hand, formation of different molybdenum species such as Mo_2C after the exposure of MoO_2 to a mixture of *n*-hexane/hydrogen mixture during the catalytic reaction was not observed at the experimental conditions employed in this work. In order to obtain such molybdenum carbide species, it is required to expose MoO_3 to a mixture of hydrocarbon-hydrogen at relatively high temperature [11]. In the case of the used metallic Mo(0) sample, the surface is partially oxidized following its exposure to air as could be deduced from the slight increase in the BE of the Mo (3d) spin-orbit components (Fig. 4b).

From the above results, it is concluded that the upper 2–3 monolayer of MoO_3 are reduced to MoO_2 at reduction temperature of 673 K with the bifunctional $MoO_2(H_x)_{ac}$ phase as the outermost surface layer. At 873 K, an important part (60%) of Mo oxide is converted to the metallic Mo(0) state on the sample surface.

3 Catalytic Results and Discussion

Systematic study of the catalytic reactions of *n*-hexane and 1-hexene will be carried out on the bifunctional $MoO_2(H_x)_{ac}$ and Mo(0) states following the procedure described in the experimental section.

3.1 The *n*-Hexane Reactant

The first catalytic activity of *n*-hexane on MoO_3/TiO_2 as a function of reduction temperature (1h) is observed at 573 K (Table 1). At this temperature, only 0.5% of *n*-hexane is converted to 2- and 3 methyl pentane isomers, which is attributed to the partial reduction of the surface MoO_3 to MoO_2 as characterized by UPS. At 623 K reduction temperature, the conversion is increased to 25.9% while the isomerization selectivity decreases to 79%. The same trend is observed in which the conversion increases with increasing the reduction temperature up to 673 K. This increase in the conversion corresponds to the conversion of the majority, if not all, of the surface to the MoO_2 phase. In order to make sure that the sample surface is completely converted to MoO_2, the catalyst sample is maintained under hydrogen at 673 K for 12 h. A conversion of 97.6% with only 25.7% in 2 and 3MP isomerization

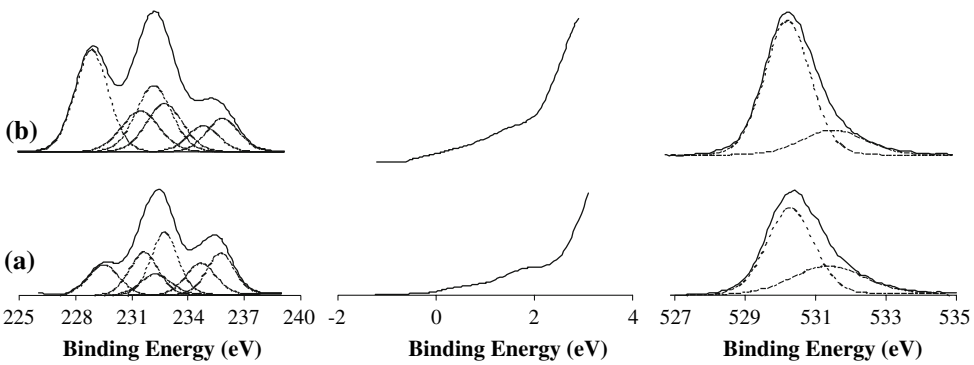

Fig. 4 The XPS-UPS spectra of the Mo (3d), O1s and VB energy regions used catalysts, (**a**) the bifunctional $MoO_2(H_x)_{ac}$ system (**b**) the metallic Mo(0) state

Table 1 Catalytic reactions of *n*-hexane on MoO_3/TiO_2 as a function of reduction (reaction) temperature. At 653–673 K, the reaction temperature is 623 K

Temperature (K)	Reduction temperature					Reaction temperature after 12 h red				
	473	573	623	653	673	673	653	623	573	523
Conversion	0	0.5	25.9	61.3	76.6	97.6	93.2	80.9	42.2	0
Selectivity, %	0	100	79.0	72.7	71.3	25.7	41.4	76.3	96.0	0
Cracking, %	0	0	21.0	27.3	28.7	74.3	58.6	23.7	4.0	0
2MP/3MP	0	0.8	1.6	1.6	1.5	1.4	1.4	1.5	1.8	0
2,2 DMB/2,3 DMB	0	0	0.2	0.3	0.4	1.3	1.1	0.7	0.4	0
Distribution of branched isomer, %										
iC4	0	0	2.2	2.6	2.9	10.5	8.2	2.9	0	0
iC5	0	0	1.3	2.0	2.7	7.2	8.6	4.4	0.9	0
2,2 DMB	0	0	2.0	2.4	2.9	1.1	3.0	5.5	2.8	0
2,3 DMB	0	0	8.4	7.4	7.4	0.9	2.7	7.7	7.8	0
2MP	0	43.9	40.3	36.1	33.6	3.5	11.1	33.3	54.4	0
3MP	0	56.1	24.8	22.2	21.8	2.6	7.7	22.4	30.1	0
Distribution of cracked products, %										
C1	0	0	0.1	0.1	0.2	2.4	1.6	0.5	0	0
C2	0	0	1.2	1.3	1.3	10.8	6.6	1.8	0	0
C3	0	0	16.9	22.1	23.0	43.9	36.1	15.5	2.4	0
C4	0	0	2.2	2.3	2.5	13.0	9.5	3.3	0.7	0
C5	0	0	0.9	1.4	1.6	4.1	4.8	2.6	0.9	0

products were obtained at 673 K reaction temperature (Table 1). Central C3–C3 bond cleavage seems to be the dominant catalytic process at this reaction temperature. It is interesting to note that at 623 K reaction temperature, the conversion 80.9% as compared to only 25.9%, obtained at the beginning of the reduction process, while the isomerization selectivity and the 2MP/3MP ratio remain almost unchanged. The same situation is observed at 573 K with a conversion of 42.2%, compared to only 0.5% at the beginning of the reduction process. As a result, the absence on any catalytic activity of *n*-hexane at 523 K before and after the extended reduction time is most probably due to thermodynamic restriction of this catalytic reaction on the bifunctional $MoO_2(H_x)_{ac}$ phase. The catalytic performances of this Mo bifunctional phase for *n*-hexane in terms of conversion, isomerization selectivity and products distribution are comparable to the Pt based catalyst deposited on zeolites [2].

Different catalytic behavior was observed following prolonged sample exposure to hydrogen at 873 K for more than 24 h (Table 2). For example, at 573 K reaction temperature, a conversion of 0.6% and 44.5% in selectivity to methyl cyclopentane was obtained. This to be compared with a conversion of 42.2% to only mono and di-branched isomers obtained in the case of $MoO_2(H_x)_{ac}$. Although the conversion increases as the reaction temperature increases to reach 100% at 873 K, different products distribution is obtained. For instance, benzene is formed at reaction temperatures between 653 and 823 K, with a maximum of 17.8% at 753 K. Toluene is also produced in much lower concentrations at reaction temperatures between 733 and 773 K (Table 2). Extensive hydrocracking to methane occurs at reaction temperatures higher than 823 K. It is important to note that in contrary to the bifunctional $MoO_2(H_x)_{ac}$ phase, mono and di-branched isomers are formed in minor quantities. Also, the 2MP/3MP ratio varies between 0.5 and 1.5 as compared to the thermodynamic equilibrium value of 1.5 observed in the case of the bifunctional system. This is due to the absence of the Brönsted Mo–OH acidic function(s) present in the bifunctional $MoO_2(H_x)_{ac}$ phase. The combination of the catalytic results and XPS-UPS characterization measurements clearly indicate that the surface which consists of $MoO_2(H_x)_{ac}$ during the gradual reduction process has been converted to the metallic Mo(0) state at 873 K reduction temperature. High electronic density of the metallic function favor benzene formation. Aromatization of *n*-hexane on Mo_2C has been reported by Solymosi et al. [11]. A conversion of $\sim$25% and $\sim$65% selectivity to benzene were obtained at 773–823 K reaction temperatures. In these experiments, molybdenum carbide has been prepared following the exposure of MoO_3 to C_2H_6/H_2 mixture at 900 K. It is well known that *n*-hexane aromatization to benzene occurs on platinum metal particles deposited on alumina or zeolite(s) [12, 13]. It was also found that the selectivity for benzene increases as a

Table 2 Products distribution of *n*-hexane at different reaction temperatures on partially reduced MoO_3/TiO_2 at 873 K for 24 h

Reaction temperature (K)	523	553	573	623	653	673	693	713	723	733	753	773	823	873
Conversion	0.6	0.5	0.6	2.3	7.3	14.9	23.9	35.9	39.0	47.8	61.6	76.1	97.7	100
Selectivity, %	37.2	40.4	55.4	42.6	33.1	25.0	19.1	12.0	7.8	5.0	1.7	0.4	0	0
Cracking, %	62.8	59.6	44.6	57.4	66.9	75	80.9	88	92.2	95.0	98.3	99.6	100	100
2MP/3MP	0	0	0.5	1.1	1.3	1.4	1.3	1.2	1.1	0.9	0	0	0	0
2,2 DMB/2,3 DMB	0	0	0	0	0	0	0	0	0	0	0	0	0	0
Distribution of compound, %														
iC4	0	0	0	0	1.0	1.5	2.2	2.7	2.5	2.2	1.3	0.4	0	0
iC5	0	0	0	0	1.8	2.1	2.5	2.2	1.6	1.0	0.3	0	0	0
2,2 DMB	0	0	0	0	0	0	0	0	0	0	0	0	0	0
2,3 DMB	0	0	0	0	0	0	0	0	0	0	0	0	0	0
2MP	0	0	18.6	22.3	17.4	12.4	8.2	3.9	2.0	0.9	0	0	0	0
3MP	37.2	40.4	36.8	20.3	12.9	9.0	6.1	3.2	1.8	0.9	0	0	0	0
C1	0	0	0	0.9	1.3	1.5	2.2	3.3	5.3	8.2	16.2	40.6	82.3	92.8
C2	0	0	0	5.3	7.2	8.2	11.4	15.7	20.2	25.3	32.7	39.3	17.0	7.2
C3	0	0	0	14.4	17.2	17.6	21.2	23.8	23.8	22.9	17.7	9.2	0.7	0
C4	0	0	0	14.8	17.1	17.3	19.4	19.2	16.5	13.2	6.8	1.9	0	0
C5	0	0	0	13.9	12.3	10.1	9.0	6.7	4.6	2.8	1.0	0	0	0
=Cpds	0	0	0	0	8.8	18.0	13.8	10.6	9.0	5.8	2.8	0	0	0
McycloC5	62.8	59.6	44.6	8.1	1.9	0	0	0	0	0	0	0	0	0
C6H6	0	0	0	0	1.1	2.3	3.9	7.2	10.3	13.6	17.9	8.7	0	0
Toluene	0	0	0	0	0	0	0	1.6	2.4	3.2	3.2	0	0	0

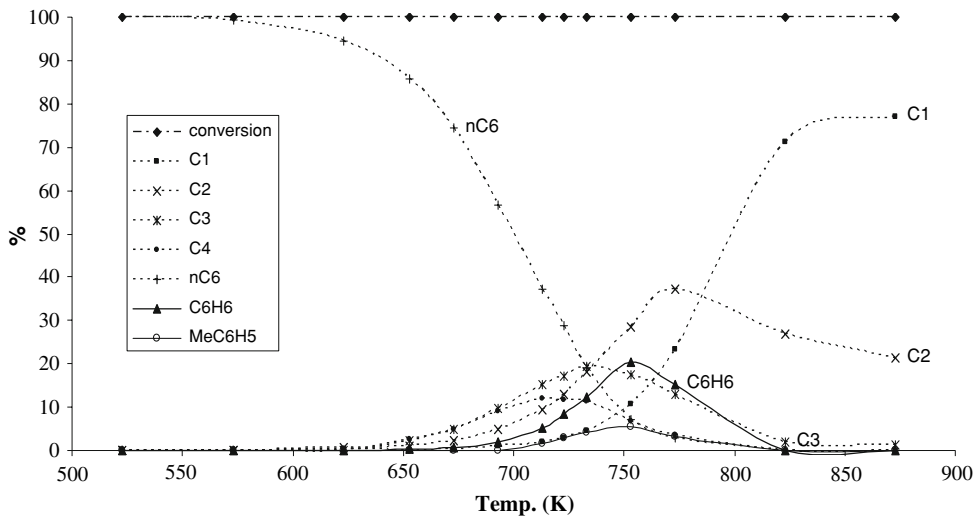

Fig. 5 Products distribution of 1-hexene as a function of reaction temperature on MoO_3/TiO_2 after reduction at 873 K for 24 h

reaction temperature increases to reach 70% at 723 K [13]. The presence of different particle size(s) formed during the catalyst preparation process and sintering problems might explains the formation of benzene as a by-product in the case of Pt based isomerization catalysts. Such particles cannot be formed in the case of $MoO_2(H_x)_{ac}$ in which the catalytic active phase consists of molybdenum atomic wire placed along the *C*-axis of the deformed rutile structure of MoO_2.

3.2 The 1-Hexene Reactant

Catalytic performances of the metallic Mo(0) surface will be further explored using 1-hexene reactant as a function of reaction temperature up to 873 K. Although similar trends to *n*-hexane are expected to be observed, the catalytic activity of the olefin will be higher since the first step which is the dehydrogenation process is already performed. In fact, we observe a 100% conversion of 1-hexene to *n*-

hexane at 523 K (Fig. 4). The same trend was observed up to 653 K at which benzene formation is initiated. At 753 K, a conversion of 100% and a selectivity of 20.4% to benzene were observed. These to be compared with 61.2% in conversion and 17.8% in selectivity obtained in the case of *n*-hexane at the same reaction temperature. As a result, it could be postulated that dehydrogenation of *n*-hexane to 1-hexene is the first catalytic process in order to form benzene on this metallic Mo(0) surface. Further work is ongoing in order to elucidate this reaction mechanism. Of note, the observed low catalytic activity of *n*-hexane at 523–653 K reaction temperatures does not necessarily correspond to the reality. A sequence of dehydrogenation of *n*-hexane to 1-hexene followed by its hydrogenation to *n*-hexane might occur with no apparent effect on the final catalytic activity of the system. It is important to note that introduction of *n*-hexane or 1-hexene without a catalyst did not show any reaction or thermal cracking at temperatures up to 873 K (Fig. 5).

4 Conclusions

Characterizations by XPS-UPS, of the equivalent 5 atomic layers of MoO_3 deposited on TiO_2 enabled us to identify the molybdenum chemical species present on the sample surface following the reduction process by hydrogen at different temperatures. At reduction temperatures between 573 and 673 K, molybdenum dioxide is formed in the upper layer, with the bifunctional (metal-acid) $MoO_2(H_x)_{ac}$ phase as the outermost surface layer. At higher reduction temperatures up to 873 K, the reduction process leads to the formation of the metallic Mo(0) state on the sample surface. Hydroisomerization of *n*-hexane to mono and di-branched compounds of relatively high octane number take place on the bifunctional $MoO_2(H_x)_{ac}$ phase at reaction temperatures between 573 and 673 K. Purely hydrogenation/dehydrogenation catalytic processes of the olefin and *n*-hexane occur on the mainly metallic Mo(0) state at low reaction temperatures. Benzene formation, in relatively low concentration, is obtained in the case of 1-hexene and *n*-hexane at reaction temperatures between 653 and 773 K on this metallic surface. This catalytic process was not observed in the case of the bifunctional $MoO_2(H_x)_{ac}$ phase.

Acknowledgments Support by Kuwait University was received through research grant # SC05/04 and SAF project GS01/01. Their support is gratefully acknowledged.

References

1. Gault F (1980) Adv Catal 30:1
2. Loften T, Blekkan EA (2006) Appl Catal A 299:250
3. Kumra T (2003) Catal Today 81:57
4. Travers C (2001) In: Leprince P (ed) 3 conversion processes, IFP Editions TECHNIP, pp 229–256
5. Katrib A, Benadda A, Sobczack JW, Maire G (2003) Appl Catal A 242:1
6. Al-Kandari H, Al-Kharafi F, Al-Awadi N, El-Dusouqui OM, Katrib A (2006) J Electron Spectrosc Relat Phenom 151:128
7. Belatel H, Al-Kandari H, Al-Kharafi F, Garin F, Katrib A (2007) Appl Catal A 318:227
8. Guilino A, Parker S, Jones FH, Egdell RG (1996) J Chem Soc Faraday Trans 12:2137
9. Pines H, Olberg RC, Ipatieff NV (1948) J Am Chem Soc 70:533
10. Zing DS, Makovsky LE, Fisher RE, Brown FR, Hercules DM (1980) J Phys Chem 84:2898
11. Solymosi F, Barthos R (2005) Catal Lett 101:235
12. Fukunaga T, Ponec V (1997) Appl Catal A 154:207
13. Philippou A, Naderi M, Pervaiz N, Rocha J, Anderson MW (1998) J Catal 178:174